PCCP

PAPER

The kinetics of folding of frataxin

Cite this: *Phys. Chem. Chem. Phys.*, 2014, **16**, 6391

Daniela Bonetti,†[a] Angelo Toto,†[a] Rajanish Giri,[a] Angela Morrone,[a] Domenico Sanfelice,[b] Annalisa Pastore,[c] Pierandrea Temussi,[d] Stefano Gianni*[ae] and Maurizio Brunori*[a]

Received 25th September 2013,
Accepted 2nd January 2014

DOI: 10.1039/c3cp54055c

www.rsc.org/pccp

The role of the denatured state in protein folding represents a key issue for the proper evaluation of folding kinetics and mechanisms. The yeast ortholog of the human frataxin, a mitochondrial protein essential for iron homeostasis and responsible for Friedreich's ataxia, has been shown to undergo cold denaturation above 0 °C, in the absence of chemical denaturants. This interesting property provides the unique opportunity to explore experimentally the molecular mechanism of both the hot and cold denaturation. In this work, we present the characterization of the temperature and urea dependence of the folding kinetics of yeast frataxin, and show that while at neutral pH and in the absence of a denaturant a simple two-state model may satisfactorily describe the temperature dependence of the folding and unfolding rate constants, the results obtained in urea over a wide range of pH reveal an intriguing complexity, suggesting that folding of frataxin involves a broad smooth free energy barrier.

1 Introduction

Frataxin is an essential mitochondrial protein involved in the metabolism of iron and responsible for the human neurodegenerative disease Friedreich's ataxia.[1] It has been shown that frataxin binds both Fe^{2+} and Fe^{3+} (ref. 2–4) and forms a ternary complex with the two main components of the iron sulphur cluster biogenesis machinery.[5] *In vitro*, the role of frataxin appears to be that of regulating the enzymatic reaction that converts cysteine into alanine to produce the sulphur which will then be incorporated into the cluster.[6] Additionally, it has been suggested to bind ferrochelatase and to participate in heme metabolism. The structure of frataxin solved by NMR[7] and crystallography[8] is highly conserved between humans, yeast and *E. coli* as shown in Fig. 1.

Recently, the folding and stability of frataxin have gained considerable attention for two quite different reasons. First, studies on yeast's frataxin have revealed that this protein undergoes cold denaturation at a temperature above 0 °C,[9–12] providing the unique possibility to address experimentally this interesting phenomenon without additives or denaturants, thus allowing an accurate assessment of the whole stability curve,[13] and a direct comparison between cold and heat denatured states.[9–12] Second, although the recessive Friedreich's ataxia is usually caused by partial silencing of the frataxin gene, 4% of the patients were found to be heterozygotes having the expansion on one allele and point mutations on the other;[14] this led to the suggestion that Friedreich's ataxia could have in some cases a misfolding component.[15,16]

In spite of being an intriguing system, no previous work has attempted to address the kinetics of folding and unfolding of frataxin, a critical task to unveil the reaction mechanism(s). Here we present a complete characterization of the kinetics of folding of frataxin, using both temperature-jump and stopped-flow experiments. As detailed below, the temperature-jump induced folding and unfolding reactions appear to be consistent with a simple two state mechanism, without the need to invoke the presence of intermediates. The experiments in urea over a wide range of pH reveal that, similarly to what was previously observed for U1A and the pleckstrin homology domain,[17,18] yeast frataxin folds *via* a mechanism involving a broad energy barrier, as mirrored by the complex dependence of the folding and unfolding rate constants on denaturant concentration.

2 Methods

Expression and purification of frataxin

Yeast frataxin protein (Yfh1) was expressed in *Escherichia coli* BL-21 (DE3) and purified by using three steps of ion-exchange

[a] *Istituto Pasteur Fondazione Cenci Bolognetti and Dipartimento di Scienze Biochimiche "A. Rossi Fanelli". Istituto di Biologia e Patologia Molecolari del CNR, Università di Roma "La Sapienza", P.le A. Moro 5, 00185, Rome, Italy. E-mail: stefano.gianni@uniroma1.it, maurizio.brunori@uniroma1.it*
[b] *Division of Molecular Structure, National Institute for Medical Research, MRC, Mill Hill, The Ridgeway, London NW7 1AA, UK*
[c] *Department of Neuroscience, Wohl Institute, King's College London, Denmark Hill Campus, London SE5, UK*
[d] *Dipartimento di Chimica, Università Federico II, via Mezzocannone 4, I-80134 Naples, Italy*
[e] *Department of Chemistry, University of Cambridge, Lensfield Road, Cambridge CB2 1EW, UK*
† D.B. and A.T. contributed equally to this work.

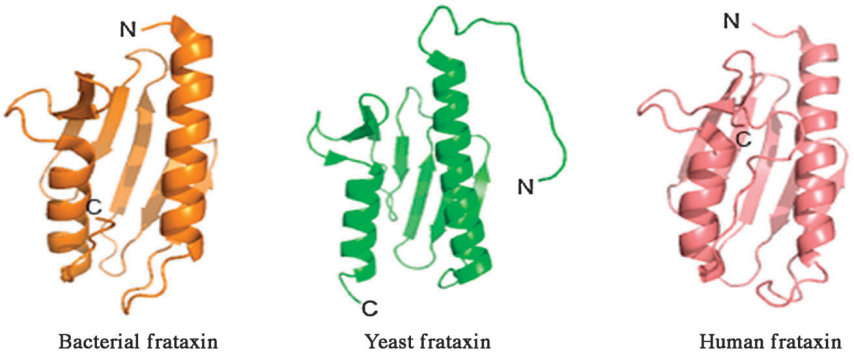

Fig. 1 Ribbon representation of the structure of frataxin orthologues. Bacterial frataxin (CyaY) is shown in orange (pdb code 1ew4), yeast frataxin (Yfh1) in green (pdb code 2ga5) and human frataxin (Hftx) in pink (pdb code 1ekg). The positions of the N and C-termini are highlighted. The structure of human frataxin comprises only the conserved domain.

chromatography: first it was used in a Q-Sepharose column (GE Healthcare) equilibrated with 25 mM Tris-HCl and 10 mM EDTA, pH 8.0. The protein was eluted with 700 mM NaCl. Then, after a buffer exchange step, the sample was loaded onto both Q and S-Sepharose columns (GE Healthcare) equilibrated with 50 mM AcOH, pH 5.0. The protein, passing through the S-column and binding to the Q-column, was eluted with 1 M NaCl. The purity of frataxin was confirmed by SDS-PAGE.

Equilibrium experiments

Thermal denaturation was followed on a JASCO circular dichroism (CD) spectropolarimeter (JASCO, Inc., Easton, MD), in a 1 mm quartz cuvette[13] at 222 nm. Protein concentration was typically 10 μM. The buffers used were 20 mM sodium acetate from pH 4.0 to 5.0, 20 mM sodium phosphate pH 6.2, 20 mM Hepes from pH 7.0 to pH 8.0 and 20 mM CHES from pH 8.5 to 9.0. All the experiments were performed in the presence of 20 mM KCl and 2 mM DTT.

Temperature-jump fluorescence spectroscopy

The relaxation kinetics were measured by using a Hi-Tech PTJ-64 capacitor-discharge T-jump apparatus (Hi-Tech, Salisbury, UK). Temperature was rapidly changed with a jump-size of 9 K. Usually 10–20 individual traces were averaged. The fluorescence change of *N*-acetyltryptophanamide (NATA) was used in control measurements. Degassed and filtered samples were slowly pumped through the 0.5 × 2 mm quartz flow cell before data acquisition. The excitation wavelength was 296 nm and the fluorescence emission was measured using a 320 nm cut-off glass filter. Protein concentration was typically 10 μM. The buffer used was 20 mM Hepes, 20 mM KCl and 2 mM DTT at pH 7.0.

Stopped-flow measurements

Kinetic folding experiments were carried out on a single-mixing SX-18 stopped-flow instrument (Applied Photophysics, Leatherhead, UK); the excitation wavelength was 280 nm and the fluorescence emission was collected using a 320 nm cut-off glass filter. Protein concentration was typically 1 μM.

3 Results

Equilibrium measurements

The thermal denaturation profile of yeast frataxin monitored by far-UV CD spectroscopy in 20 mM Hepes pH 7.0, in the presence of 20 mM KCl and 2 mM DTT, is shown in Fig. 2. In agreement with previous reports, we observed a pronounced cold denaturation phase, the protein regaining ellipticity at temperatures below 295 K. Because thermal denaturation typically occurs in a limited window of temperatures, it is generally very difficult to measure experimentally the change in heat capacity upon unfolding, Δc_p, which is related to the amount of hydrophobic area that becomes solvent exposed upon unfolding.[19] In the case of frataxin, the direct observation of cold denaturation was previously employed to estimate a value of 1790 ± 40 cal mol^{-1} K^{-1} from CD and NMR data.[9] Alternatively, the change in heat capacity can be estimated, according to Fersht,[20] from the dependence of ΔH_{Tm} and T_m at different pHs, returning a value of $\Delta c_p = 1220 \pm 70$ cal mol^{-1} K^{-1}. Both values appear to be compatible with what is expected from the change in accessible surface area upon unfolding of a globular

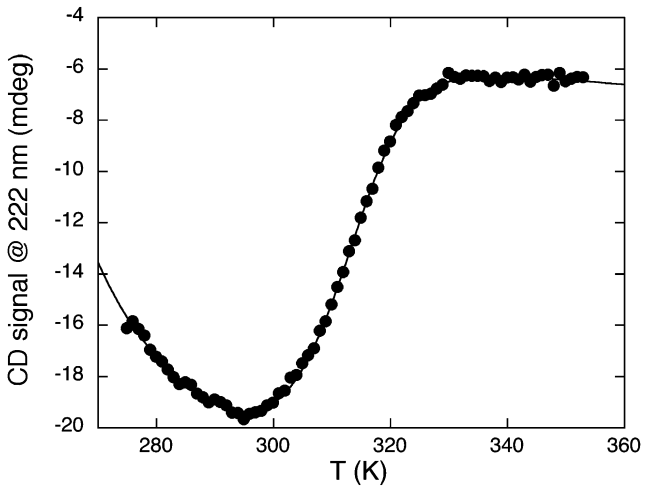

Fig. 2 Thermal denaturation profile of yeast frataxin obtained in 20 mM Hepes pH 7.0 in the presence of 20 mM KCl and 2 mM DTT, monitored by far UV circular dichroism (CD) over the range 275–353 K.

protein of about 100 folded residues.[19] However, the difference between these two values probably arises from the assumption that whilst a direct fit of the thermal profile assumes the structure of the denatured state to be unaffected by changes in temperatures, the dependence of ΔH_{Tm} and T_m at different pHs assumes the enthalpy of protonation of glutamate and aspartate groups in the protein to be negligible. It should be noted, however, that the numerical difference between the two estimates had little effects on the calculation of the overall protein stability ΔG_{D-N}. Thus, to a first approximation, we have used the value of 1220 ± 70 cal mol^{-1} K^{-1} to calculate the stability parameter, ΔG_{D-N} for thermal denaturation as a function of temperature and to deconvolute the folding and unfolding rate constants from relaxation kinetics (see below).

Temperature-jump experiments

To measure the kinetics of heat-induced folding and unfolding directly, we carried out temperature-jump experiments which are similar in design and methodology to what was previously reported for barstar.[21] In particular, the protein sample in the presence of 20 mM Hepes at pH 7.0 was subjected to a rapid increase in temperature of 9 K using a capacitor discharge temperature-jump apparatus.[22–24] In order to ensure sample conductivity, all experiments (including equilibrium) were carried out in the presence of 20 mM KCl, even if it has been reported that salts significantly increase stability and eventually can make cold denaturation unobservable above water freezing.[9,10] The initial equilibrium temperature was varied systematically from 279 to 324 K, in order to monitor both the folding (from 279 to 285 K) and unfolding (from 290 to 324 K) reactions. Two typical temperature-jump induced refolding and unfolding time-courses are reported in Fig. 3. It is evident that whilst at the higher starting temperatures a rapid increase in temperature leads to unfolding of the protein, as mirrored by a decrease in fluorescence emission, at lower temperatures the folding reaction was observed. In all cases (but particularly at lower temperatures where the overall relaxation event is slower) a drift in the fluorescence is observed after the transition, reflecting cooling of the sample.

The temperature dependence of the reciprocal relaxation time k_{obs} is reported in Fig. 4. An analysis of the kinetic folding mechanism of frataxin as a function of temperature demands deconvolution of the folding and unfolding rate constants. Because the reciprocal relaxation time is equal to the sum of the rate constants for the forward and reverse reactions at the final temperature, we calculated the folding (k_F) and unfolding[25] rate constants by using the thermodynamic parameters obtained from equilibrium thermal denaturation experiments (see above). The following equations were employed:

$$K_{D-N}(T) = e^{\Delta G_{D-N}(T)/RT} \quad (1)$$

$$K_{D-N}(T) = \frac{k_F(T)}{k_U(T)} \quad (2)$$

$$k_{obs} = k_F(T) + k_U(T) \quad (3)$$

where K_{D-N} represents the equilibrium constant, T the absolute temperature in Kelvin, ΔG_{D-N} the free energy change for the folding reaction and R the universal gas constant.

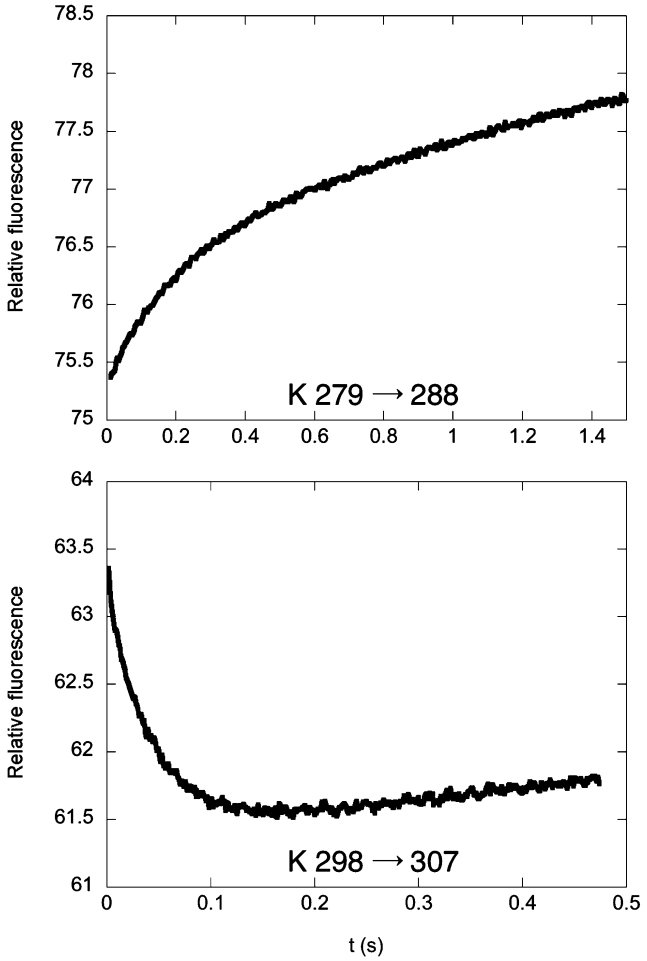

Fig. 3 Time course of temperature-jump induced refolding (top panel) and unfolding (bottom panel) obtained by a 9 K increase in temperature, starting from an initial equilibrium value of 279 K for refolding and of 298 K for unfolding. The change in fluorescence emission seen at the lower starting temperature (top) is consistent with refolding of the protein, whilst at the higher starting temperature (below) the unfolding reaction is observed.

In analogy to what was previously observed for barnase,[26] it is evident that at temperatures above 310 K, folding displays a negative activation enthalpy, the folding rate constant decreasing with increase in temperature. This effect is due to the high dimensional nature of the protein folding reaction, which is driven by the formation and breakage of many weak noncovalent interactions between the macromolecule and the solvent. Negative activation enthalpy has been classically interpreted as a reflection of the transient breakage of the water icebergs surrounding the hydrophobic regions of the denatured polypeptide.[20,25,27]

According to transition state theory,[28] the dependence of the activation free energy on temperature can be described as follows:

$$\Delta G^{TS}(T) = \Delta H^{TS}(T_0) - T\Delta S^{TS}(T_0) + \Delta c_p^{TS}\left[(T - T_0) - T\ln\frac{T}{T_0}\right] \quad (4)$$

where ΔH^{TS} is the activation enthalpy, T is the absolute temperature in Kelvin, T_0 is a temperature of reference, ΔS^{TS} is the activation

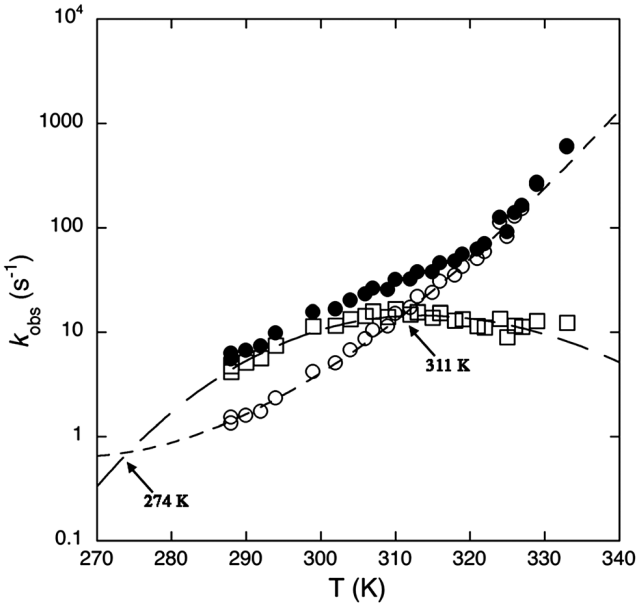

Fig. 4 Temperature dependence of the observed reciprocal relaxation time k_{obs} (●) measured by temperature jump. Deconvolution of k_{obs} into k_F (□) and k_U (○) using K_{D-N} derived from equilibrium measurements (Fig. 2) is shown together with respective fits (dashed lines). The arrows indicate the two melting mid-temperatures for the cold and the hot denaturation.

entropy and Δc_p^{TS} is the change in heat capacity. Furthermore, by applying Eyring's equation[29] to the folding and unfolding rate constants the following equations may be derived:

$$k_F = \varepsilon \frac{k_B}{h} e^{\left[\Delta S_F^{TS}(T_0)\right]/R} T e^{\left\{-\Delta H_F^{TS}(T_0) - \Delta c_{p,F}^{TS}\left[(T-T_0) - T \ln \frac{T}{T_0}\right]\right\}/RT} \quad (5)$$

and

$$k_U = \varepsilon \frac{k_B}{h} e^{\left[\Delta S_U^{TS}(T_0)\right]/R} T e^{\left\{-\Delta H_U^{TS}(T_0) - \Delta c_{p,U}^{TS}\left[(T-T_0) - T \ln \frac{T}{T_0}\right]\right\}/RT} \quad (6)$$

where ε is the transmission coefficient, k_B is Boltzmann's constant, h is Plank's constant and ΔS_F^{TS}, ΔH_F^{TS}, and $\Delta c_{p,F}^{TS}$ are the change in entropy, enthalpy and heat capacity of folding, respectively, while ΔS_U^{TS}, ΔH_U^{TS}, and $\Delta c_{p,U}^{TS}$ are the change in entropy, enthalpy and heat capacity of unfolding.

A quantitative analysis by following the two-state equations reported above is shown in Fig. 4. The two points of intersection between the curves representing the temperature dependence of k_F and k_U (see arrows) correspond to the two melting temperatures for the cold and the hot denaturation, 274 K and 311 K, respectively. A quantitative analysis of the folding and unfolding rate constants allows to calculate the total change of Δc_p as the sum of $\Delta c_{p,F}^{TS} + \Delta c_{p,U}^{TS}$. The resulting value of 1.20 ± 0.67 kcal mol^{-1} K^{-1} is in satisfactory agreement with the total Δc_p obtained by equilibrium experiments 1.22 ± 0.07 kcal mol^{-1} K^{-1}. This agreement suggests the folding–unfolding kinetics of yeast frataxin at pH 7.0 to conform to a two-state mechanism involving a single transition state,[30] over a wide range of temperatures.

Kinetic experiments in urea

The study of the denaturant dependence of folding demands the stability of the protein to be sufficiently high to allow a complete analysis of the folding and unfolding rate processes. In fact, because the observed kinetics results from the linear combination between the forward and reverse rate constants, a quantitative analysis can only be performed when both the refolding and unfolding components may be characterized over a wide range of denaturant concentrations. Thus, since frataxin is marginally stable (*i.e.* $\Delta G_{D-N} = 0.64 \pm 0.03$ kcal mol^{-1} at 298 K), we resorted to measure its folding and unfolding kinetics under stabilizing conditions, *i.e.* in the presence of 0.4 M sodium sulfate. Furthermore, because of the dependence of frataxin stability on ionic strength, we selected urea, rather than guanidine hydrochloride, as a chaotropic denaturant.

The folding and unfolding kinetics of yeast frataxin were investigated over a large range of pH, ranging from 4.0 to 9.0. In all cases, the time course was fitted satisfactorily to a single exponential decay at any final urea concentration; each rate constant was obtained from the average of at least five independent shots in stopped-flow experiments. The semi-logarithmic plots of the observed folding–unfolding rate process of frataxin *versus* denaturant concentration (chevron plots) at the different pH values are presented in Fig. 5. Whilst in the absence of sodium sulfate we could detect only the unfolding arm of the chevron plot (data not shown), in the presence of a stabilizing salt well-defined V-shaped chevron plots were seen under all conditions. Remarkably, however, it is evident that the chevron plots display a pronounced curvature

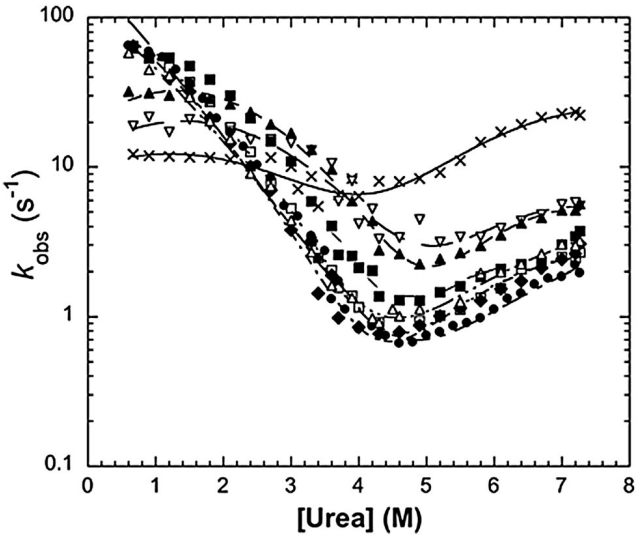

Fig. 5 Semi-logarithmic plot of the observed rate constants for folding and unfolding of frataxin *versus* [urea] measured by stopped flow at 298 K, in the presence of 0.4 M sodium sulfate, at different pH values (×, pH 4.0; ▽, pH 4.5; ▲, pH 5.0; ■, pH 5.5; □, pH 6.0; ●, pH 7.0; ♦, pH 8.0; △, pH 9.0). Lines are the best fit to a mechanism involving the presence of a broad energy barrier.

in both the folding and unfolding arms. To a first approximation, therefore, data recorded in urea appear to suggest that frataxin does not conform to a simple two-state folding,[30] but demands a more complex description.

The presence of curvatures in chevron plots has been interpreted by different models. Classically, a deviation from linearity in the unfolding or refolding limb was attributed to the presence of an intermediate in the reaction pathway. In this case, a complexity may either arise from the rapid accumulation of such an intermediate[31,32] or by a change in the rate limiting step with changing denaturant concentration.[33] However, alternative explanations have been put forward, such as the presence of a broad transition state separating the native and the denatured states.[18] Whilst these different models are often experimentally indistinguishable, a kinetic test has been recently proposed to discriminate between the different scenarios.[17] In particular, by analyzing the robustness of the observed curvature with changing reaction conditions, it is possible to reconstruct the transition state shifts as a function of protein stability over a wide stability range, to screen for fingerprints more sensitive for different barrier profiles. In practice, the test is performed by fitting the observed chevron plot to the following quadratic equation:

$$k_{\mathrm{obs}} = k_{\mathrm{F}}^{\mathrm{w}} \mathrm{e}^{\left(m_{\mathrm{F}}[\mathrm{denaturant}]+m'[\mathrm{denaturant}]^2\right)} + k_{\mathrm{U}}^{\mathrm{w}} \mathrm{e}^{\left(m_{\mathrm{U}}[\mathrm{denaturant}]+m'[\mathrm{denaturant}]^2\right)} \quad (7)$$

where $k_{\mathrm{F}}^{\mathrm{w}}$ and $k_{\mathrm{U}}^{\mathrm{w}}$ represent the folding and unfolding rate constants in water, m_{F} and m_{U} are the respective slopes of the folding and unfolding arms and the degree of curvature of the chevron plot is reported by the parameter m' (which tends to 0 for a perfectly V-shaped, two-state, chevron plot). Then, by measuring the robustness of m' with changing reaction conditions (for example, by changing the pH), it is possible to conclude whether or not the rate limiting barrier conforms to a smooth broad energy profile. In the case of frataxin, as depicted in Fig. 5, a global analysis of the chevron plots with a shared value of m' returned an excellent fit. This observation indicates that, in analogy to what was observed for U1A and the pleckstrin homology domain,[17] the curvature in frataxin is very robust to changes in experimental conditions and suggests the protein to fold *via* a broad smooth free energy barrier.

4 Discussion

Frataxin is a mitochondrial protein critical for the metabolism of iron. The discovery of its role in the pathophysiology of Friedreich's ataxia in humans as well as the recent observation of a pronounced cold denaturation phenomenon in the absence of osmolytes explain why this protein may be considered as a very good system for protein folding studies.

In this work we have extensively characterized the temperature and urea dependence of the kinetics of folding of yeast frataxin both in the absence and in the presence of a stabilizing salt. Data reveal that the observed dependence of the relaxation time measured by temperature-jump experiments between 288 and 333 K appears to be consistent with a simple two state process involving a single energy barrier. On the other hand, the experiments carried out using urea as a chaotropic denaturant and exploring a very wide pH range (4 to 9) highlight an additional complexity of the folding of frataxin, suggesting the main rate limiting step to conform to a smooth broad free energy barrier. In order to reconcile these apparently contrasting results we observe that whilst in temperature-jump experiments a relatively small change in stability is imposed, with a $\Delta\Delta G = 2.1 \pm 0.06$ kcal mol^{-1} when varying the temperature from 288 to 330 K, increasing the urea concentration from 0 to 8 M involves more pronounced changes, with a $\Delta\Delta G = 11.4 \pm 0.5$ kcal mol^{-1}. Therefore, the changes in stability involved in temperature jump experiments are most likely too small to perturb the folding of the protein sufficiently to detect changes in rate determining steps. Thus, while the data recorded in urea require a more complex description, a simple two-state model may satisfactorily describe the temperature dependence of the folding and unfolding rate constants.

It is of interest to discuss the significance of broad energy barriers in protein folding. In fact, while many globular proteins appear to fold *via* a robust transition state, whose structures are not affected by changes in experimental conditions (or denaturant concentration), in a few cases, such as U1A,[34] azurin[35] and yeast frataxin, a broad barrier, implying a malleable structure, may be more adequate to account for the data. Wolynes and co-workers[35] suggested this behaviour to arise from the presence of strained energetics in the native state ensemble, namely, energetic frustration. Because of this complexity, these systems are of particular interest from an experimental perspective, as they may provide information on both the early and late events of folding, as well as the continuum of states in between. This aim is generally not possible with simple two-state folders, where the main transition state represents a single ''snapshot'', which may be characterised.[36] Nevertheless, it should be recalled that in experiments carried out in bulk, the behaviour of individual molecules cannot be addressed, the experimental information reporting the average properties. Therefore, whilst the characterization of broad barrier folders may provide a sequence of events leading the (wide) denatured ensemble to the (narrower) native state(s), only the average structural features arising from multiple parallel pathways may be inferred. Thus, the only experimental method to address the sequence of events of folding is the analysis of the transition paths for single molecules, as shown by Eaton and co-workers.[37,38]

One of the critical questions in the protein folding is to address the role of residual structure of denatured states in dictating folding pathways.[39–42] Indeed, ever since the pioneering work of Ptitsyn,[43,44] it was suggested that the overall three-dimensional topology of proteins may form before the tight packing of the side chains. This view led to the hypothesis that a 'molten globule' intermediate may exist in the folding pathway. This state typically displayed some conserved features, such as a roughly globular shape, a significant content of secondary structure and the lack of a well-defined tertiary structure.[45,46] Thus, a two-state folding behaviour may be reconciled with the 'molten globule'

concept assuming the denatured state to retain some residual structure under physiological conditions. Furthermore, it should be stressed that both the denatured and native states represent an ensemble of different quasi-iso-energetic structures in rapid equilibrium.[47] Recent studies on proteins displaying nearly identical amino acid sequences but different folds and functions appear to suggest that the topology of a folded protein is already pre-sculpted in its denatured state.[48] This recent observation highlights the need for addressing the residual structure of denatured states, which is still centre stage in the protein folding field. Yet, because of their elusive nature, it is very difficult to unveil directly the residual structure of denatured ensembles as it is necessary to destabilize the native state without the addition of chemical denaturants. In this perspective, the hot and cold denatured states of frataxin, recently characterized using a combination of NMR and SAXS techniques[11] seem to display differences in the radius of gyration and in the residual content of secondary structure. Therefore, characterizing the molecular mechanism of both the hot and cold denaturation of frataxin offers the tantalizing possibility to infer directly the role of residual structure in the denatured state in dictating folding processes. Within this frame, the kinetic analysis presented in this paper aims to set the scene for deeper analysis of the molecular mechanism of folding of frataxin under different experimental conditions, *i.e.* starting from different denatured states. Future work based on protein engineering and Φ value analysis will shed light on the role of residual structure of the frataxin's denatured state in dictating its folding pathway.

Acknowledgements

This work was partly supported by grants from the Italian Ministero dell'Istruzione dell'Universita e della Ricerca (Progetto di Interesse 'Invecchiamento' to S.G.), Sapienza University of Rome (C26A13T9NB to S.G.) and EMBO (to S.G.).

References

1 A. Pastore and H. Puccio, *J. Neurochem.*, 2013, **126**, 43–52.
2 S. Adinolfi, M. Trifuoggi, A. S. Politou, S. Martin and A. Pastore, *Hum. Mol. Genet.*, 2002, **11**, 1865–1877.
3 Y. He, S. L. Alam, S. V. Proteasa, Y. Zhang, E. Lesuisse, A. Dancis and T. L. Stemmler, *Biochemistry*, 2004, **43**, 1625–1626.
4 M. Nair, S. Adinolfi, C. Pastore, G. Kelly, P. Temussi and A. Pastore, *Structure*, 2004, **12**, 2037–2048.
5 F. Prischi, P. V. Konarev, C. Iannuzzi, C. Pastore, S. Adinolfi, S. R. Martin, D. I. Svergun and A. Pastore, *Nat. Commun.*, 2010, **1**, 95.
6 S. Adinolfi, C. Iannuzzi, F. Prischi, C. Pastore, S. Iametti, S. R. Martin, F. Bonomi and A. Pastore, *Nat. Struct. Mol. Biol.*, 2009, **16**, 390–396.
7 G. Musco, G. Stier, B. Kolmerer, S. Adinolfi, S. Martin, T. Frenkiel, T. Gibson and A. Pastore, *Structure*, 2000, **15**, 695–707.
8 S. Dhe-Paganon, R. Shigeta, Y. I. Chi, M. Ristow and S. E. Shoelson, *J. Biol. Chem.*, 2000, **275**, 30753–30756.
9 A. Pastore, S. R. Martin, A. Politou, K. C. Kondapalli, T. Stemmler and T. PA, *J. Am. Chem. Soc.*, 2007, **129**, 5374–5375.
10 M. Adrover, V. Esposito, G. Martorell, A. Pastore and P. A. Temussi, *J. Am. Chem. Soc.*, 2010, **132**, 16240–16246.
11 M. Adrover, G. Martorell, S. R. Martin, D. Urosev, P. V. Konarev, D. I. Svergun, X. Daura, P. Temussi and A. Pastore, *J. Mol. Biol.*, 2012, **417**, 413–424.
12 S. R. Martin, V. Esposito, P. De Los Rios, A. Pastore and P. A. Temussi, *J. Am. Chem. Soc.*, 2008, **130**, 9963–9970.
13 W. J. Becktel and J. A. Schellman, *Biopolymers*, 1987, **26**, 1859–1877.
14 M. Pandolfo and A. Pastore, *J. Neurol.*, 2009, **256**, 9–17.
15 A. R. Correia, S. Adinolfi, A. Pastore and C. M. Gomes, *Biochem. J.*, 2006, **398**, 605–611.
16 A. R. Correia, C. Pastore, S. Adinolfi, A. Pastore and C. M. Gomes, *FEBS J.*, 2008, **275**, 3680–3690.
17 S. Gianni, M. Brunori, P. Jemth, M. Oliveberg and M. Zhang, *Biochemistry*, 2009, **48**, 11825–11830.
18 M. Oliveberg, *Acc. Chem. Res.*, 1998, **31**, 765–772.
19 J. K. Myers, C. N. Pace and J. M. Scholtz, *Protein Sci.*, 1995, **4**, 2138–2148.
20 A. Fersht, *Structure and mechanism in protein science*, Freeman W. H. and Co, New York, 1999.
21 B. Nolting, R. Golbik and A. R. Fersht, *Proc. Natl. Acad. Sci. U. S. A.*, 1995, **92**, 10668–10672.
22 G. Czerlinski and M. Eigen, *Z. Elektrochem.*, 1959, **63**, 652–661.
23 M. Eigen and G. G. Hammes, *J. Am. Chem. Soc.*, 1960, **82**, 5951–5952.
24 M. Eigen and G. G. Hammes, *Adv. Enzymol. Relat. Areas Mol. Biol.*, 1963, **25**, 1–38.
25 P. L. Privalov, Y. Griko, S. Y. Venyaminov and V. P. Kutyshenko, *J. Mol. Biol.*, 1986, **190**, 487–498.
26 M. Oliveberg, Y. J. Tan and A. R. Fersht, *Proc. Natl. Acad. Sci. U. S. A.*, 1995, **92**, 8926–8929.
27 P. L. Privalov, *Crit. Rev. Biochem. Mol. Biol.*, 1990, **25**, 281–305.
28 S. Arrhenius, *Z. Phys. Chem.*, 1889, **4**, 226–248.
29 H. J. Eyring, *J. Chem. Phys.*, 1932, **3**, 107–115.
30 S. E. Jackson and A. R. Fersht, *Biochemistry*, 1991, **30**, 10428–10435.
31 S. Khorasanizadeh, I. D. Peters and H. Roder, *Nat. Struct. Biol.*, 1996, **3**, 193–205.
32 M. J. Parker, J. Spencer and A. R. Clarke, *J. Mol. Biol.*, 1995, **253**, 771–786.
33 F. Khan, J. I. Chuang, S. Gianni and A. R. Fersht, *J. Mol. Biol.*, 2003, **333**, 169–186.
34 T. Ternstrom, U. Mayor, M. Akke and M. Oliveberg, *Proc. Natl. Acad. Sci. U. S. A.*, 1999, **96**, 14854–14859.
35 C. Zong, C. J. Wilson, T. Shen, P. Wittung-Stafshede, S. L. Mayo and P. G. Wolynes, *Proc. Natl. Acad. Sci. U. S. A.*, 2007, **104**, 3159–3164.
36 A. R. Fersht, *Proc. Natl. Acad. Sci. U. S. A.*, 2000, **97**, 1525–1529.
37 H. S. Chung and W. A. Eaton, *Nature*, 2013, **502**, 685–688.

38 H. S. Chung, K. McHale, J. M. Louis and W. A. Eaton, *Science*, 2012, **335**, 981–984.
39 E. R. McCarney, J. E. Kohn and K. W. Plaxco, *Crit. Rev. Biochem. Mol. Biol.*, 2005, **40**, 181–189.
40 T. L. Religa, J. S. Markson, U. Mayor, S. M. Freund and A. R. Fersht, *Nature*, 2005, **437**, 1053–1056.
41 W. F. van Gunsteren, R. Bürgi, C. Peter and X. Daura, *Angew. Chem., Int. Ed.*, 2001, **40**, 351–355.
42 K. B. Wong, J. Clarke, C. J. Bond, J. L. Neira, S. M. Freund, A. R. Fersht and V. Daggett, *J. Mol. Biol.*, 2000, **296**, 1257–1282.
43 O. B. Ptitsyn, *Adv. Protein. Chem.*, 1994, **47**, 83–229.
44 O. B. Ptitsyn, *Nat. Struct. Biol.*, 1996, **3**, 488–490.
45 O. B. Ptitsyn, *Curr. Opin. Struct. Biol.*, 1995, **5**, 74–78.
46 O. B. Ptitsyn, V. E. Bychkova and V. N. Uversky, *Philos. Trans. R. Soc., B*, 1995, **348**, 35–41.
47 H. Frauenfelder, S. G. Sligar and P. G. Wolynes, *Science*, 1991, **254**, 1598–1603.
48 A. Morrone, M. E. McCully, P. N. Bryan, M. Brunori, V. Daggett, S. Gianni and C. Travaglini-Allocatelli, *J. Biol. Chem.*, 2011, **286**, 3863–3872.